Available online at www.sciencedirect.com
ScienceDirect
Ceramics International 38 (2012) 65–75
CERAMICS INTERNATIONAL
www.elsevier.com/locate/ceramint

Hydrogen sulfide sensing properties of multi walled carbon nanotubes

Nosrat Izadi [a], Ali Morad Rashidi [a,*], Samira Golzardi [a], Zeinab Talaei [b], Ali Reza Mahjoub [b], Mir Hassan Aghili [a]

[a] Nano Technology Center, Research Institute of Petroleum Industry, Tehran, Iran
[b] Department of Chemistry, Faculty of Science, Tarbiat Modares University, Tehran, Iran

Received 13 March 2011; received in revised form 15 June 2011; accepted 17 June 2011
Available online 24th June 2011

Abstract

This paper investigates the effect of functional groups on the hydrogen sulfide sensing properties of multi-walled carbon nanotubes using carboxyl and amide groups and Mo and Pt nanoparticles as decorated precursors in gaseous state at working temperature. Carbon nanotubes were synthesized by the CVD process and decorated with the nano particles; provide higher sensitivity for H_2S gas detection. The MWCNTs were characterized by scanning electron microscopy combined with energy dispersive X-ray (SEM/EDX), transmission electron microscopy (TEM), X-ray diffraction (XRD), ATR-IR absorption and Fourier transforms infrared (FT-IR) analyses. The MWCNTs were deposited as a thin film layer between prefabricated gold electrodes on alumina surfaces. The sensitivity of carbon nanotubes was measured for different H_2S gas concentrations and at working temperature. The results showed that the measured electrical conductance of the modified carbon nanotubes with functional groups is modulated by charge transfer with P-type semiconducting characteristics and metal decorated carbon nanotubes exhibit better performances compared to functional groups of carboxyl and amide for H_2S gas monitoring at room temperature.

Keywords: E. Sensors; Hydrogen sulfide; Multi walled carbon nanotubes

1. Introduction

Measurement represents one of the oldest methods used by human beings to better understand and control the world. These measurements are often accomplished using a singular sensor or an array of sensors [1]. Thus sensors that can detect gaseous molecules in industrial, medical, and living environments are in great demand nowadays [2–7]. Many of the gas sensors that are made of semiconducting oxide materials such as SnO_2, TiO_2, In_2O_3 and ZnO are based on the changes in electrical resistance of the materials upon gas adsorption [8,9]. In the sensor structures, the principle naturally requires a larger surface-area-to-volume ratio for high sensitivity; for this matter, thin films and porous thick films have been extensively studied. Recently, nanostructures, such as carbon nanotubes (CNTs), with extremely high surface-area-to-volume ratios, have begun attracting wide attention in the study of their application to various sensors [10]. Carbon nanotubes are a class of advanced functional materials that have many applications. They are essentially two different types of carbon nanotubes, namely the metallic nanotubes and the semiconducting nanotubes [11]. In addition, these tubes can be either single-walled or multi-walled [12]. Carbon nanotubes have outstanding properties associated to unusual structural such as electrical, optical, mechanical and thermal characteristics. These properties are essential to make them the most promising candidates for many potential applications in nanotechnology. One of their main applications is in the field of gas sensors [13–16]. The electronic property of SWCNTs is determined by their size and chirality. The conductivity of each layer of MWCNTs behaves like an SWCNT along the axial direction, while it is very poor between the layers. As a whole, most MWCNTs display good conductivity. The unique electronic property combining with others makes carbon nanotubes ideal building block for electronic devices such as quantum wires, diodes, field-effect transistors (FETs), sensors, and cold cathode field emitters [17]. Also, the carbon nanotubes are considered ideal building blocks for gas adsorption and chemical gas sensing due to their long specific surface area, hollow geometry, nanosized structure, including high electrical mobility of the charge-carriers in

* Corresponding author. Tel.: +98 2148252323; fax: +98 2144739696.
E-mail address: Rashidiam@ripi.ir (A.M. Rashidi).

0272-8842/$36.00 © 2011 Published by Elsevier Ltd and Techna Group S.r.l.
doi:10.1016/j.ceramint.2011.06.038

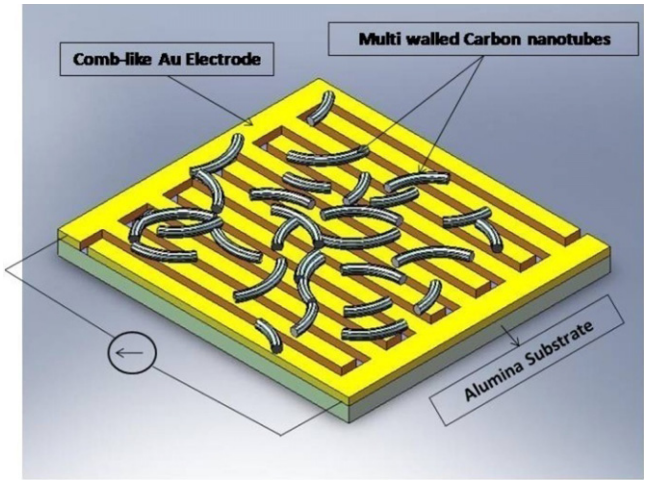

Fig. 1. Schematic view of sensor based on MWCNTs networked films.

defect-free nanostructures [18–23]. It has been demonstrated that CNTs can be used to detect low concentrations of gases with maximum performance in terms of high sensitivity, fast response and good repeatability. But the sensing mechanisms involved are not fully understood. Recently, gas sensors based on functionalized carbon nanotubes have been proposed capable of detecting small gas concentrations with high specificity [24–34]. In this study, sensors based on networked CNTs-bundle nano materials, grown by catalytic chemical vapor decomposition process and functionalized with carboxyl, amide and nanoclusters of Pt and Mo have been investigated for environmental monitoring applications of H_2S at working temperature.

2. Experimental

2.1. Preparing of gas sensors

Fig. 1 shows the schematic of the sensing device, which consists of an Al_2O_3 substrate with dimensions of (10 mm × 10 mm × 1 mm), a pair of gold interdigitated electrodes with 20 fingers (350 μm spacing, 5 mm length and 350 μm width) that was prepared by a lithography technique and a gas sensing layer. Multi walled carbon nanotubes were prepared by a enhanced chemical vapor deposition over a Co–Mo supported MgO nanoporous catalyst at a reasonably temperature of 1173 K, consisting of high purity methane (99.999%) as carbon source in a 1.5 m horizontal two pass-fixed-bed tubular (quartz) reactor placed in a 100 cm long and programmable tubular furnace with 90–95% purity by our groups as described elsewhere [35]. The average diameters of nano tubes vary from 40 to70 nm and their length from 5 to 15 μm. To enhance the functionalization of MWCNTs with carboxyl group, these tubes were sonicated at 60 °C with a solution of HNO_3 (65% purity) and H_2SO_4 (98% purity) (3:1, v/v) for 3 h. These tubes were also functionalized with amide ($CONHC_{18}H_{37}$) group by our workers as described elsewhere [36]. Incipient impregnation process was used for Mo decoration of carbon nanotubes using $(NH_4)_6Mo_7O_{24}{\cdot}4H_2O$ as precursor. Metal precursor $(NH_4)_6Mo_7O_{24}$ with desired amount of 1 wt% Mo was added to some water depending on the pore size of the support and impregnated to the CNT support and dried at 70 °C and finally calcined at 500 °C for 2 h in N_2 flow. Pt/CNT-COOH nano material was prepared by alcohol reduction in the presence of acetate anions as stabilizing agents (a new method). Ethanol was used as both the reducing agent and the solvent. First carbon nanotubes were immersed in a mixture of concentrated sulfuric and nitric acids (98% and 65%, v/v, 3:1), and sonicated in an ultrasonic bath, keeping the temperature at 60 °C for 3 h. After filtration, the obtained black solids were washed several times with pure water and dried. Then oxidized carbon nanotubes were dispersed in diluted ethanol solution (2:1, v/v, ethanol/water) in the presence of sodium acetate as stabilizing agent. Then $H_2PtCl_6.6H_2O$ was added to the nanotubes suspension followed by refluxing at 85 °C in ultrasonic bath. After the reaction was done and cooled to room temperature, the solid material was obtained by filtration, washed with water and dried at 80 °C in an oven overnight. The crystalline structure of carbon nanotubes was characterized by XRD, SEM/EDX, TEM, ATR-IR and FT-IR analyses. At the beginning of fabricating the gas sensors, 1 mg of the as-prepared MWCNTs bundles were dispersed in 30 ml of ethanol by ultrasonic vibration for about 3 h to obtain the well-mixed suspensions. Then, the suspensions were coated onto the surfaces of the Au comb electrodes and the Al_2O_3 substrate by spin coating. The spinning was at 800 rpm and the period of coating was 20 s. Thereafter the coating layers were heated in air using an oven at approximately 150 °C for 30 min, to evaporate the solvents in the coating layers. The gas detection apparatus (Fig. 2) comprised of gas suppliers, mass flow controllers, a detector unit, a U-like quartz glass reactor with a diameter of 2.5 cm and a length of about 150 cm and a jacket heater. Data acquisition system was performed by means of an A/D board and GAS4 software. The DC electrical measurement was made using an applied voltage of 5.00 V onto a known resistance in series with the sensor. The DC electrical conductance of the MWCNTs-sensors during the gas exposures has been measured by the volt-amperometric technique. The CNT based sensor was installed in the glass reactor and connected to the detector unit via signal wires to record the resistance changes of the thin films vs time. In this study, H_2S gas was used as the detecting gas. During gas sensing, small amounts of H_2S gas were carried by air or N_2 into the glass reactor through the mixer. Gas-sensing tests were performed at room temperature (20 °C) through 250 °C, and the total flow rate of the H_2S and the carrier gas was kept constant at 200 $cm^3\ min^{-1}$ in each test. Various concentrations of the H_2S gas were produced by modulating the ratio of the flow rate of H_2S gas to that of the carrier gas. The initial resistance (R_{air}) was measured in dry air at test temperature. The measurement of the electrical resistance–time response patterns of the element to various concentrations of H_2S gas was carried out at test temperature. After exposed to sensing gas for 5 min, the sensor was put in rapidly in air flow and the resistance variation was observed and recorded.

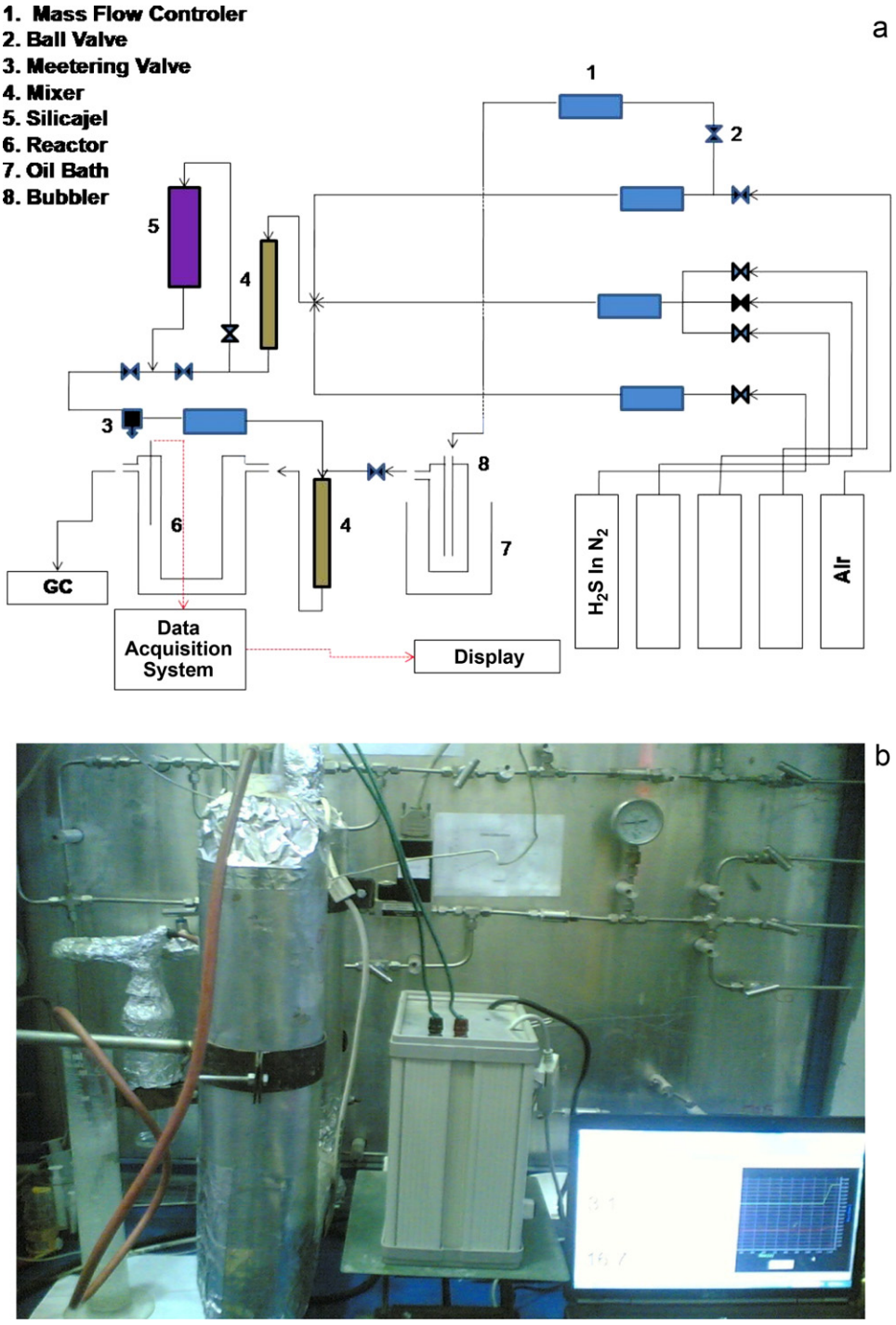

Fig. 2. (a) Schematic set up used for gas sensing testing of MWCNTs networked films. (b) Experimental set up used for gas sensing testing of MWCNTs networked films.

3. Results and discussion

3.1. CNTs characterization

The crystalline structure of carbon nanotubes was characterized by XRD, SEM/EDX, TEM, ATR-IR and FT-IR analyses. The X-ray diffraction (XRD) pattern of samples was recorded on a PW-1840 X-ray diffract meter (Philips), using Cu-K_α (1.5 Å) radiation operated at 40 kV and 30 mA. The SEM/EDX images were obtained with a Cambridge S-360 operated at 16 kV and 2.5 μA and XL-30 energy dispersive X-ray (Philips). The EDX instrument can only detect the content of metal in the sample no content of carbon. The TEM photographs were obtained with a LEO-912-AB operated at 85 kV. The ATR analysis of the experiment was performed by a Bruker ISS-88 instrument and the FT-IR spectra was recorded on Perkin Elmer Spectrum-GX. Figs. 3–7 display SEM/EDX, TEM, XRD, FT-IR and ATR analyses of these materials,

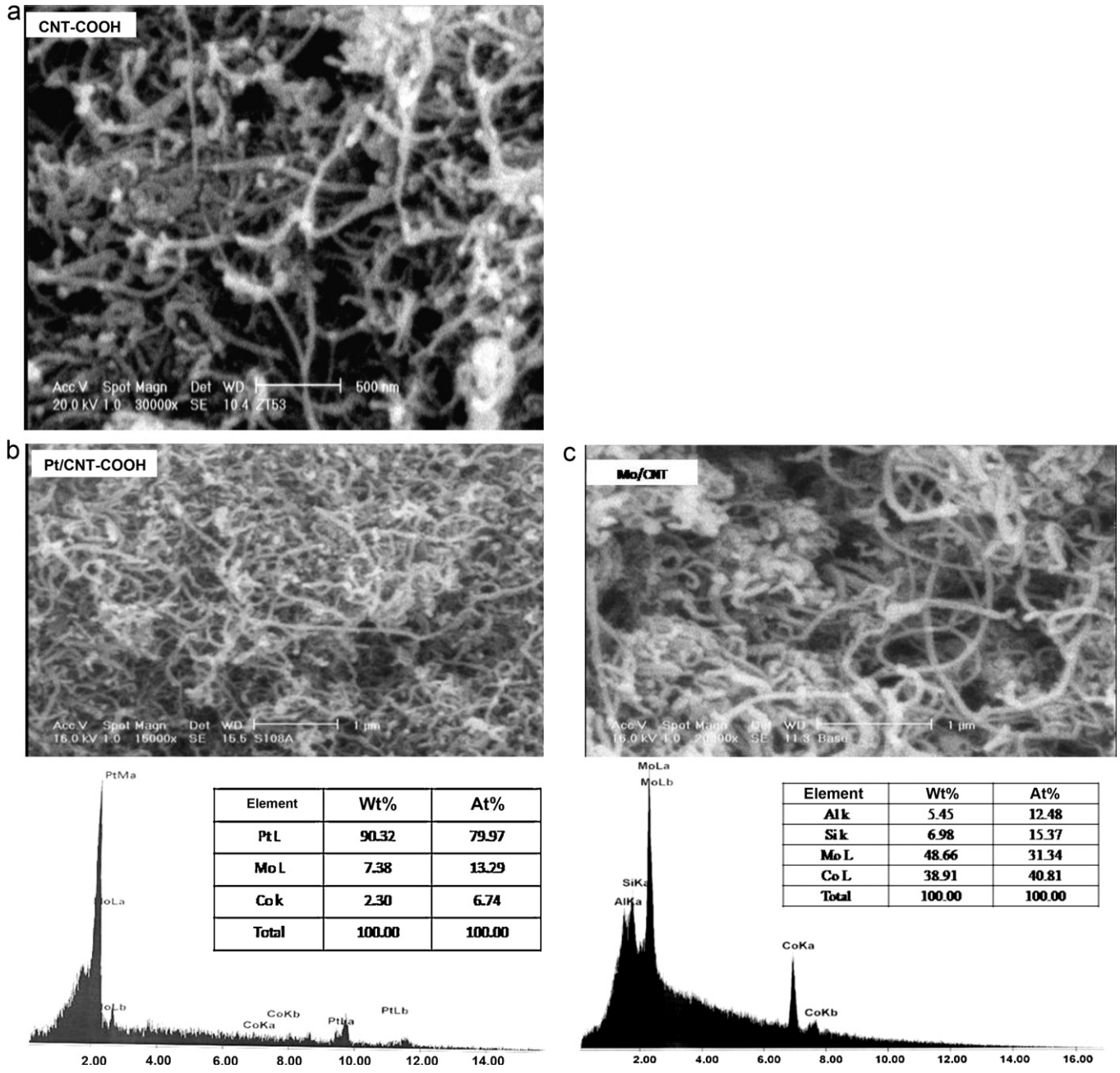

Fig. 3. SEM/EDX images of the prepared MWCNTs with various decorations (a) CNT-COOH, (b) Pt/CNT-COOH, and (c) Mo/CNT.

respectively. Fig. 3a shows the SEM image of the MWCNTs sample with functionalization of carboxyl group. Fig. 3b and c shows the SEM/EDX images of various modifications of carbon nanotubes with Pt and Mo nanoparticles as decorated precursors prepared by the different method. Fig. 4a and b presents the TEM micrographs of the MWCNTs loaded 1 wt% of metal nanoparticles. Fig. 5a–c shows the XRD pattern of MWCNTs with decoration of Pt, Mo nanoparticle and amide group. As shown in Fig. 5a and b X-ray diffraction analysis of both Pt/CNT-COOH and Mo/CNT catalysts reveals the graphitized nature of carbon in the CNT support that is confirmed by the presence of C (0 0 2) and C (1 0 0) reflections at 2θ close to 26 and 40, respectively. Deposition of platinum or molybdenum species on CNT support and reduction of catalyst precursors led to the formation of Pt^0 or MoO_3 phases that cannot be detected by means of the XRD technique in 1 wt% loading. The broadening of diffraction peaks is too large to identify Pt or MoO_3 nanoparticles in the Pt/CNT-COOH or Mo/CNT catalysts. Fig. 6 shows FT-IR spectra for the CNT-$CONHC_{18}H_{37}$ based sensors. In Fig. 6 the spectrum of carboxylated MWNTs, peak at 1636 cm^{-1} corresponds to amido-functionalized MWNTs. The ATR analysis of the experiment was presented in Fig. 7. As shown in Fig. 7 the band around 1569 is attributed to the graphitic structure of MWCNTs. The presence of carboxylic C=O (~1720 cm^{-1}), C–O (~1199 cm^{-1}) and OH (~2400–3400 cm^{-1}) vibrations in the spectrum of oxidized MWCNTs indicated that carboxyl groups are introduced to the tip and sidewalls of the MWCNTs.

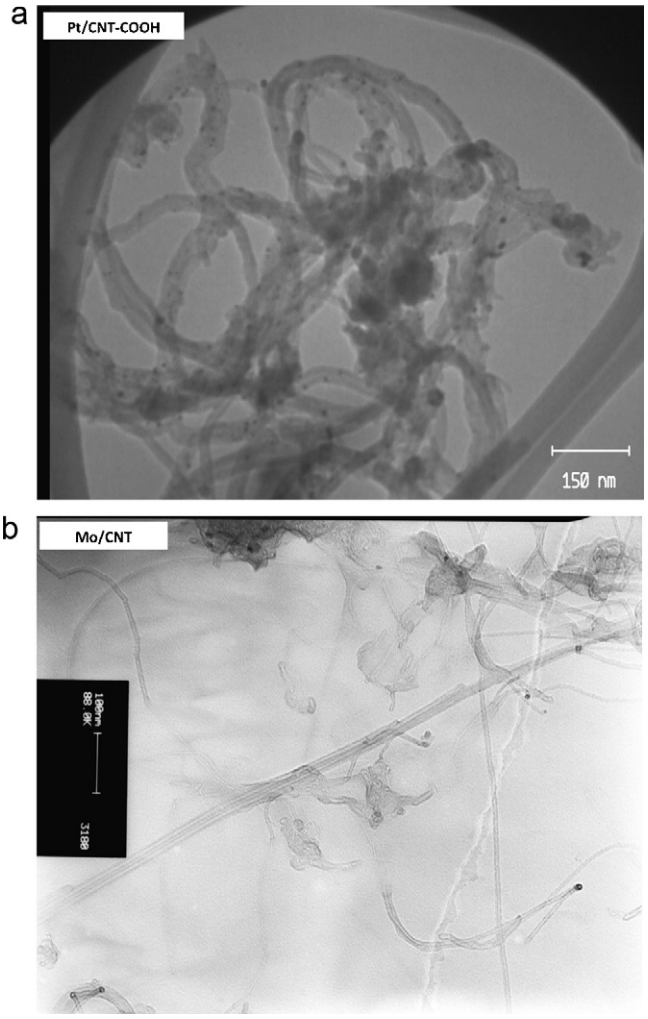

Fig. 4. TEM images of bundles of decorated of CNTs thin films (a) Pt/CNT-COOH and (b) Mo/CNT.

3.2. Resistance measurements with H_2S gas at room temperature

To compare the sensing characteristics of the sensors CNTs-based devices, at working temperature, the gas sensor response (S) is defined as Eq. (1) [37–39]:

$$S(\Omega) = R_s(\Omega) - R_{air}(\Omega) \quad (1)$$

where R_s is the resistance of sensor upon test gas concentration, and R_{air} is the resistance of sensor upon dry air. The resistance of the CNT-based sensors was measured in varying H_2S concentrations 10,000–200 ppm balanced with the N_2 carrier gas. The device was allowed to equilibrate for 1 h before H_2S gas was introduced. The initial resistance of these sensors was kept around 1.8 kΩ. The net gas flow was set at 200 cm^3 min^{-1} for all experiments. Fig. 8 shows the response curve of sensing materials of Mo/CNT, Pt/CNT-COOH, CNT-$CONHC_{18}H_{37}$ and CNT-COOH at room temperature to 1500 ppm H_2S. The output resistance depicts the rise from the background resistance R_{air} to the value R_s that occurs when the H_2S gas enters the test reactor. In all experiments the response time was kept at 5 min. For tested device, this time is not to obtain a result equal to 100% of the equilibrium signal. On the other hand, during time 5 min, it was allowed the H_2S gas passes over the device, after it, the gas flow was off, thus the response time larger than $t = 5$ min needs for the steady state of sensor in pollutant gas. As shown in Fig. 8, the sensor resistance monotonously increases after H_2S gas exposure but the recovery behaviors are very poor at room temperature. Poor recovery time at room temperature for H_2S sensors based on CNTs has been reported by A.I.Y. Tok et al. [40]. They suggested that the long recovery time is due to a strong bonding between H_2S and Ag nanoparticles. Also recovery time longer than 12 h for the NO_x sensors based on CNTs has been reported by Kong et al. [18]. Such a long recovery is due to a strong bonding energy between NO_x molecules and CNTs sites [41]. The recovery time of gas desorption can be expressed by the Arrhenius form of $\tau = \nu_0^{-1} \exp(-E_B/k_B T)$ [41], where E_B is the adsorption energy, T is the absolute temperature, k_B is the Boltzmann's constant, and ν_0 is the attempt frequency. The theoretical calculation of adsorption energy between NO_2 and SWNTs is about 0.6 eV and does not clearly depend on the diameter and chirality of SWNTs [42]. With E_B, k_B, and ν_0 as the constants for a given gas specie, the recovery time will decrease at high temperatures. The rapid recovery time for H_2S gas sensors based on CNTs at 200 °C has been reported by Penza et al. [27]. The observed behavior of explained sensors in above was also created in the H_2S gas sensors based on CNTs in this study, i.e., the response curve and the recovery behavior of the Pt-CNT-COOH based sensor to 1500 ppm H_2S at room temperature have been shown in Fig. 9. The initial resistance of sensor in air was around 1.38 kΩ. The sensor response estimated from Fig. 9 was 300 Ω increase exposure to H_2S for 5 min and 20 Ω decrease according to air ($t = 30$ min). In the second step these values were reduced to 60 and 20 Ω to H_2S and air, respectively. Table 1 and Fig. 10 compares only the responses to 200–10,000 ppm H_2S of MWCNTs with different modifications of carboxyl and amide groups and Pt and Mo nanoparticles at room temperature.

3.3. Gas sensing mechanism of MWCNTs-based sensors

3.3.1. CNT-COOH, CNT-$CONHC_{18}H_{37}$ and Pt/CNT-COOH based sensors

As presented in Fig. 8 in all experiments a p-type semiconductor response to H_2S gas is observed, i.e., an increase in resistance in the presence of a reducing gas for four-type sensors based on Mo/CNT, Pt/CNT-COOH, CNT-COOH and CNT-$CONHC_{18}H_{37}$. As presented in Fig. 10 the CNTs-based sensors show lower response at the low concentration (200 ppm). However, as the H_2S concentration increases, the CNTs-based sensors demonstrate larger response. In general, on increasing the gas concentrations, the responses depend on. Also, the electrical resistance of the unmodified and metal modified CNTs-based sensors specifically increases upon individual gas exposure of the reducing gas (H_2S) due to molecules adsorption. The adsorption of electron-donating (H_2S) gas molecules in the networked CNTs bundles causes

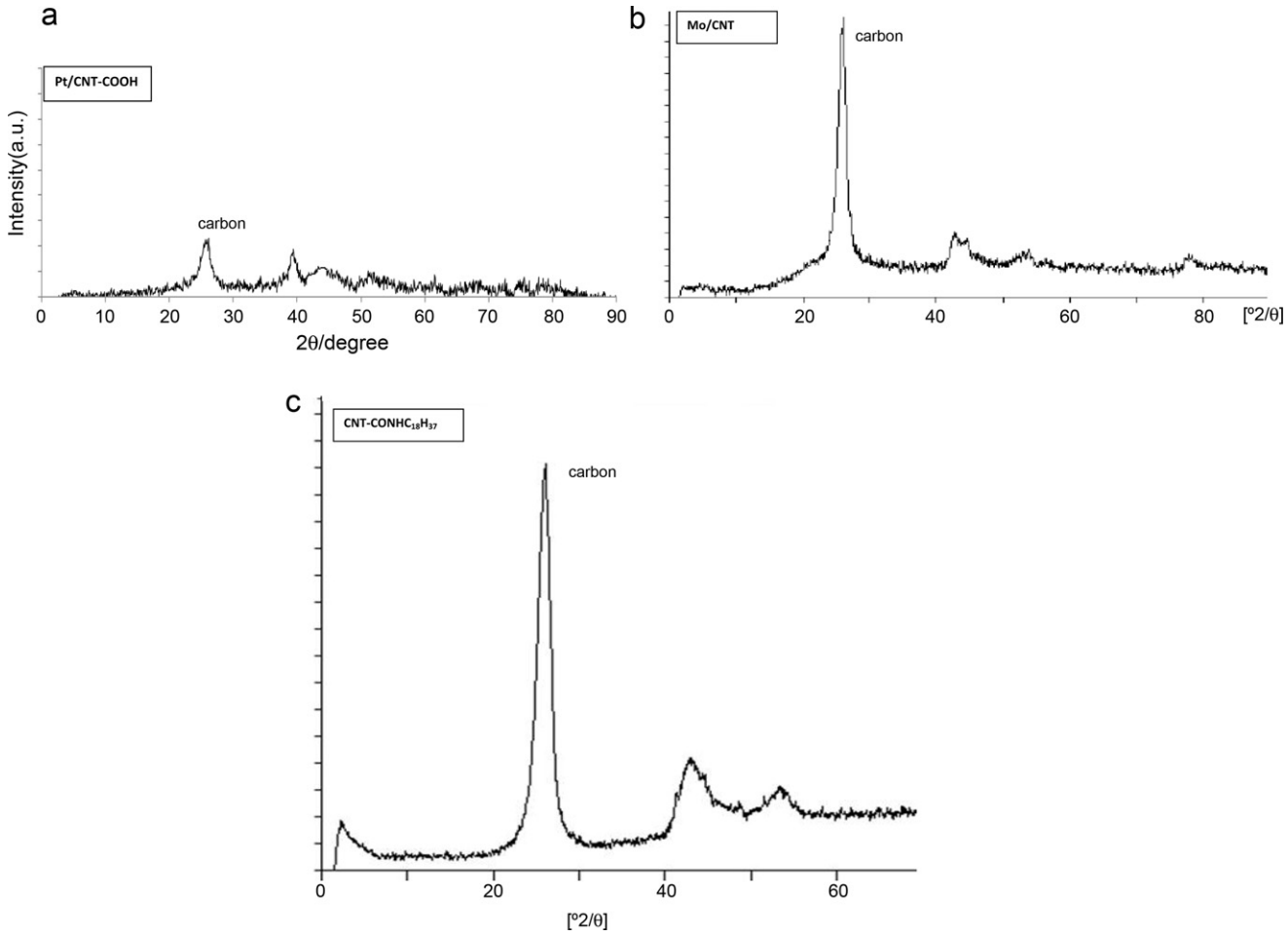

Fig. 5. X-ray diffraction patterns of decorated MWCNTs with (a) Pt, (b) Mo nanoparticles and (c) amide group.

charge transfer between the CNTs-based nano material and the gas molecules. Thus, the adsorption of electron-donating (H_2S) gas causes the number of holes in valence band to decrease and Fermi level is shifted from valence band and thus increasing the electrical resistance [27]. This trend of the sensor gas response is observed for both unmodified and metal modified CNTs. These results clearly demonstrate a p-type semiconducting behavior of the CNTs bundles. This p-type characteristic is also observed after the carboxylic acid, amide and the metal functionalization of the CNTs-bundles. The p-type behavior of the metal-functionalizated CNTs may significantly affect the binding affinity and sticking coefficient of the electron-donating gases to the nanotubes. As shown in Table 1 at room temperature, the Mo/CNT, CNT-COOH, CNT-$CONHC_{18}H_{37}$ and Pt/CNT-COOH sensors show a response *S* of 310.24, 205.2, 224.8 and 306.3 Ω to 200 ppm H_2S gas and 805.9, 291, 392.9 and 539.5 Ω to 1500 ppm H_2S gas, respectively. The difference in gas response between unmodified and metal-functionalized of carbon nanotubes in all concentrations of H_2S gas is observed. The Mo/CNT and CNT-COOH based sensors exhibit the highest and the lowest of sensitivity, respectively. Wu [38] presented that carboxylic acid (–COOH) produced on the surface of carbon nanotubes increases the adsorption sites for CO gas, whilst, in this study, this trend is not observed for H_2S gas. The lower sensitivity of CNT-COOH based sensor in the sensing of H_2S gas probably is due to the interaction of carboxylic acid groups and acidic property of sulfide hydrogen. Desorption of two acidic groups hinders access of the H_2S molecules to the surface sites. CNT-$CONHC_{18}H_{37}$ based sensor exhibit a response *S* of 224.8 Ω to 200 ppm H_2S gas higher than carboxylic acid at room temperature. This property probably is related to basic property of CNT-$CONHC_{18}H_{37}$ based sensor

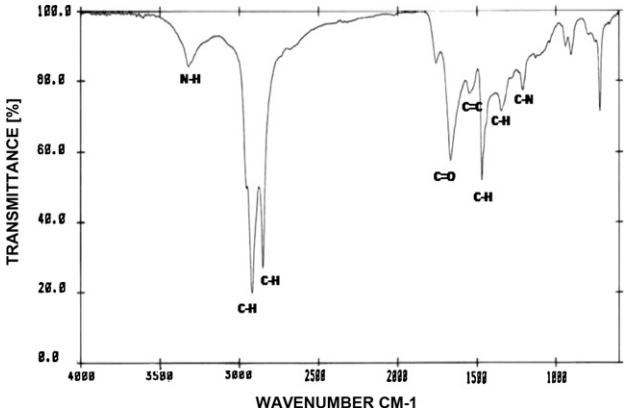

Fig. 6. FT-IR spectra of functionalized MWCNTs with amide groups.

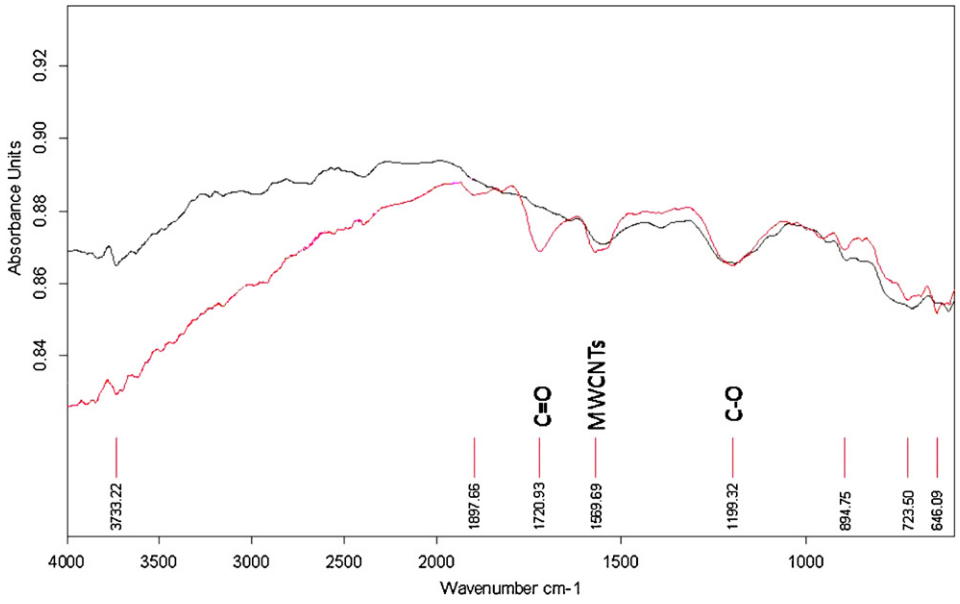

Fig. 7. The ATR spectra of MWCNTs functionalized with carboxyl group.

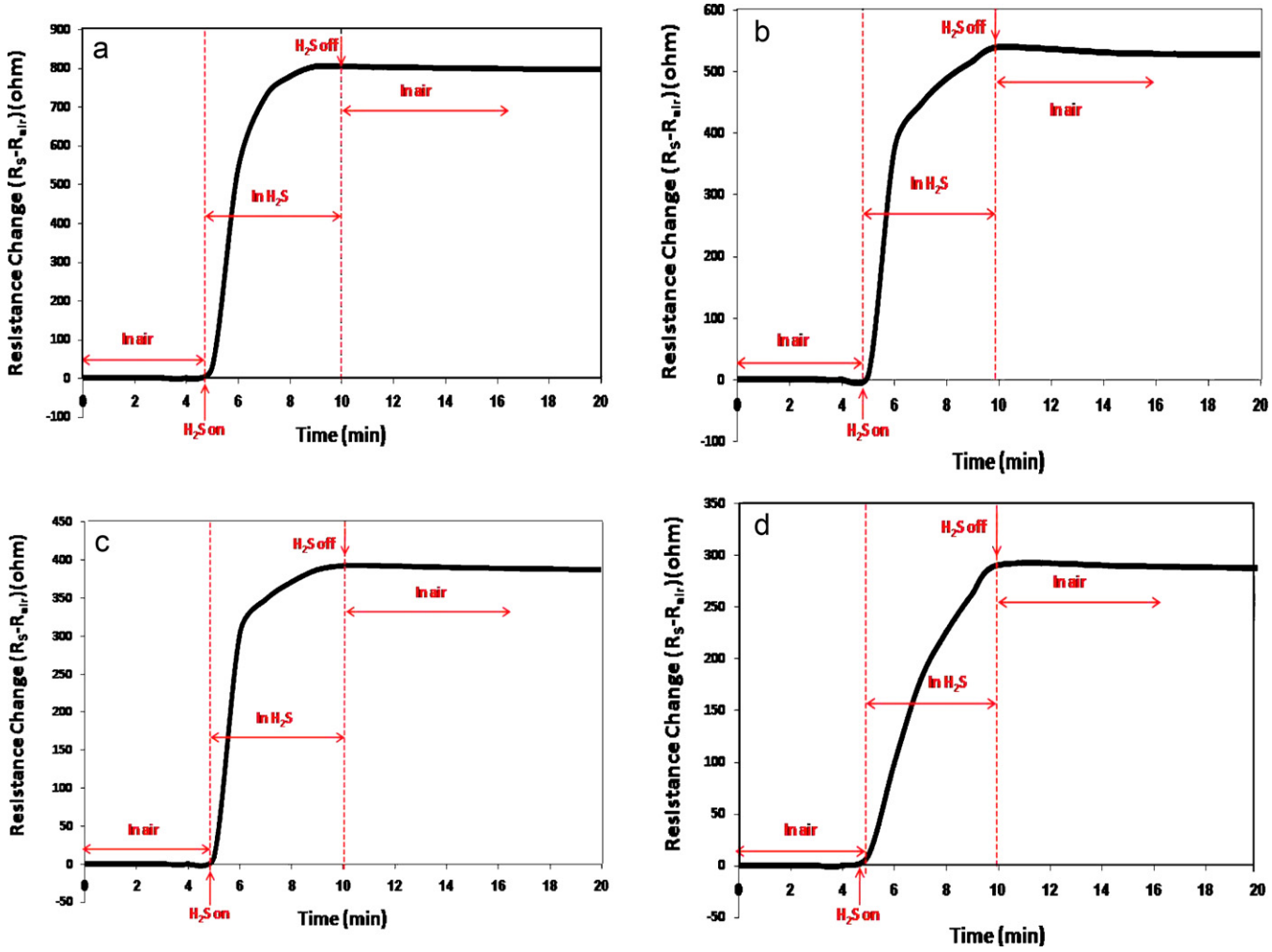

Fig. 8. Response curves of (a) Mo/CNT, (b) Pt/CNT-COOH, (c) CNT-CONHC$_{18}$H$_{37}$, and (d) CNT-COOH based sensors to 1500 ppm H_2S gas at room temperature.

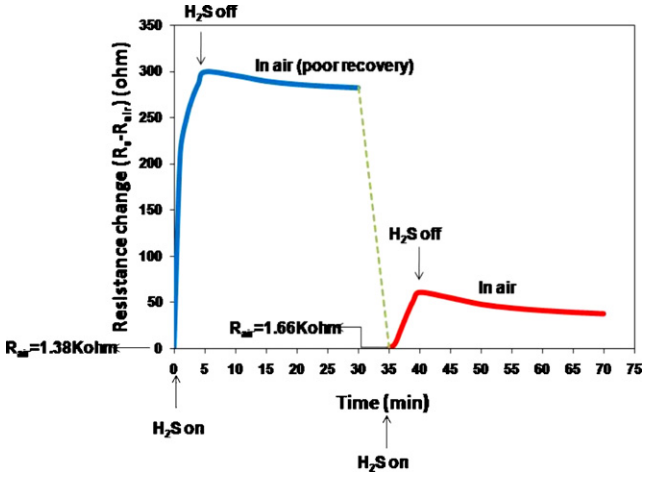

Fig. 9. Response curve and reproducibility of Pt/CNT-COOH based sensor with recovery time to 1500 ppm H_2S gas at room temperature.

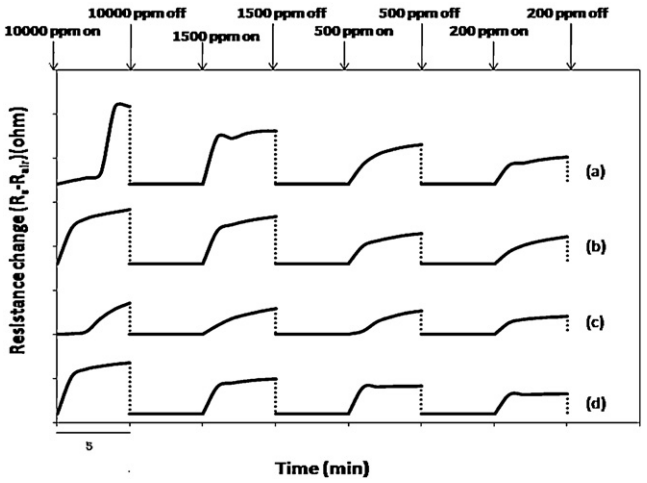

Fig. 10. The time response in terms of electrical resistance changes for sensors based on (a) Mo/CNT, (b) Pt/CNT-COOH, (c) CNT-COOH, and (d) CNT-$CONHC_{18}H_{37}$ in the presence of different H_2S gas concentrations at room temperature.

with amide groups and adsorption properties of acidic and basic materials. However, it can be observed that for metal-functionalized CNTs, the addition of proper nano metal leads to an increment in the sulfide hydrogen sensing, resulting in increasing of around 50% in sensitivity respect to undecorated carbon nanotubes. These results agree with other works [27,40] reporting that Pt or Ag-doping improves the performance of carbon nanotubes for H_2S gas. According to Penza's report [27] the enhanced effect of the metallic nanosized catalysts on gas sensitivity is strongly related to catalytic spillover at nanoclusters surface and consequent dissociation of the tested gas molecules into molecular fragments. Also, Penza [27] has been presented in his work that the molecular fragments dissolve into Pt-nanoclusters with high solubility and thus lower the work function of metals, in turn causing electron transfer from metal to nanotubes. Interface discrete states due to the charge transfer at the catalyst/nanotube contact fill the band-gap of the semiconducting CNTs. The activation energy of these gap-states depends on catalyst used, its cluster size and molecular fragments dissolved. In the case of electron-donating H_2S induced catalytic spillover, these energy levels are likely donor gap states. The donor gap states can transfer electrons to conduction band of the p-type semiconducting nanotubes with major hole-carrier by decreasing the free net charge density (e.g., increasing electron density in conduction band with unchanged hole density in valence band) and thus increasing the resistance of the sensor [27].

3.3.2. *Mo/CNT based sensor*

In 2004, Wei [43] in his report expressed that the hybrid gas sensors with SWNTs/SnO_2 nano materials exhibit much higher sensing sensitivity and recovery property in detecting NO_2 gas at room temperature than the blank SnO_2 sensor. Wei [43] compares the effect of the SWNTs in improving of gas sensing according to p^+–n/SnO_2 junctions. He explains that SnO_2 is well-known to be an n-type semiconductor. If oxidizing gas molecules (NO_2) are adsorbed onto the surface of a SnO_2 sensor, they reduce the number of the free electrons of the SnO_2, leading to the extension of the depletion zone on the SnO_2 surface, increasing the resistance of the sensor. When the oxidizing gas molecules are adsorbed as negatively charged molecules on a n-type SnO_2 sensor, forming the depletion layer on the substrate. In other hand, SWCNTs act like a p-type semiconductor when exposed to an ambient atmosphere. When SWNTs bundles in a little amount add to SnO_2 sensor with a hetero structure, two depletion layers one on the surface of the SnO_2 particles and the other in the interface between SWCNTs and SnO_2 is formed. Before the oxidizing gases are adsorbed, the widths of these two depletion layers are given by a constant value. After adsorption, the widths change to another constant value. The potential barriers at the interfaces between SnO_2 and the layer of p-SWCNTs or inside the SnO_2 layer may change. If both these effects expand the depletion layers at the

Table 1
Sensing properties of CNTs-based sensors to different concentrations of H_2S gas at room temperature.

H_2S gas (ppm)	S (Ω)			
	Mo/CNT	Pt/CNT-COOH	CNT-$CONHC_{18}H_{37}$	CNT-COOH
10,000	881.50	618.25	537.30	352.80
1500	805.90	539.50	392.90	291.00
500	450.97	338.59	315.40	267.84
200	310.24	306.30	224.80	205.20

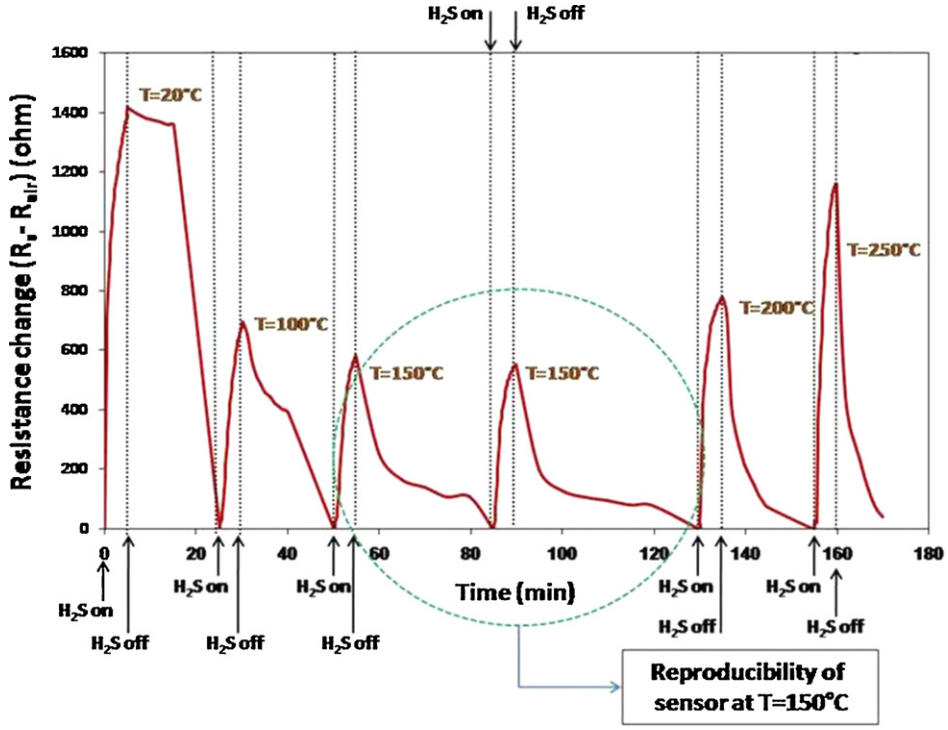

Fig. 11. Pt/CNT-COOH-based sensor response and recovery time to 1500 ppm H_2S at different testing temperatures (R_{air} = 18 kΩ).

n/p-junction of the SnO_2 substrate, then the resistances of the sensor increase upon oxidizing gas. According to expressions of Wei [43] in above, in this study, MoO_3 is also an n-type semiconductor with an oxygen deficiency. When MoO_3 is added to carbon nanotubes bundles in a little amount, two depletion layers one on the surface of the carbon nanotubes bundles and the other in the interface between CNTs and MoO_3 may be formed. In this case, the carbon nanotubes bundles play specific role and MoO_3 is added as additive promoter. Before the reducing gas (H_2S) is adsorbed, the widths of these two depletion layers are given by a constant value. After adsorption, the width of these two depletion layers change. The potential barriers at the interfaces between MoO_3 and the layer of p-MWCNTs change and this effect expands the depletion layers at the n/p-junction of the MWCNTs bundles, then the resistance of the sensor increases upon reducing gas. These trends are observed in our results.

3.4. Temperature effect and recovery characteristics

Fig. 11 shows a curve response of type Pt/CNT-COOH to cyclic exposure to 1500 ppm H_2S and air at different temperatures. The initial resistance of this type was found about 18 kΩ at room temperature. A similar result was obtained for type Pt/CNT-COOH at initial resistance of 153 Ω at $T = 20$ °C (Fig. 12). In Fig. 11 the sensor (R_{air} = 18 kΩ) was exposure to H_2S for 5 min and its resistance was increased by 1400 Ω. Here again, it can be seen that the sensor recovery after switching H_2S to air is quite slow. The recovery time for sensor in each temperature was kept at 10 min. Heating up to 100 °C would cause the decrease in resistance by 17 kΩ. After stabilizing of sensor, it again was exposure to H_2S for 5 min. The response S of type was turn out to 700 Ω. Here, it can be seen that the sensor recovery after switching H_2S to air is faster than room temperature. The sensor response S and recovery time rate for both Pt/CNT-COOH based sensors have been illustrated in Table 2.

The data in Figs. 11 and 12 and Table 2 demonstrate that the sensor response of Pt/CNT-COOH does not exhibit from the smooth increasing or decreasing trend by increasing of the working temperature. The sensor response is relatively high at room temperature, but i.e., for sensors with initial resistances of 18 kΩ and 150 Ω it decreases from 1416.80 Ω to 580.30 Ω and

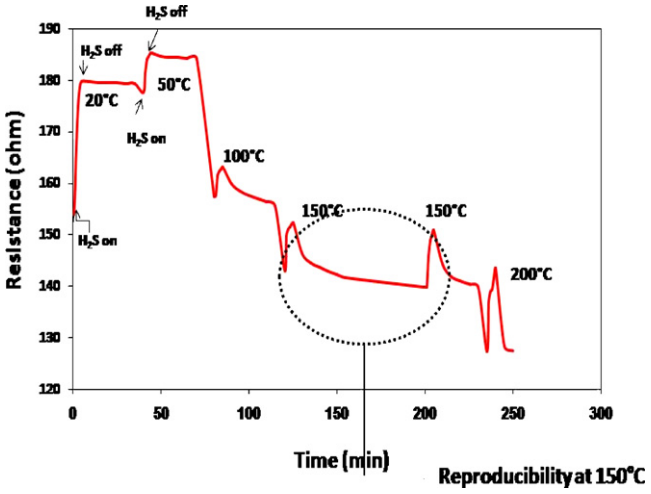

Fig. 12. Pt/CNT-COOH-based sensor response and recovery time to 1500 ppm H_2S at different testing temperatures (R_{air} = 150 Ω).

Table 2
Sensor response and rate of regeneration of Pt/CNT-COOH at different working temperatures to 1500 ppm H_2S.

Working temperature (°C)	S (Ω)		Rate of recovery (Ω/min)	
	R_{air} = 18 kΩ	R_{air} = 150 Ω	R_{air} = 18 kΩ	R_{air} = 150 Ω
20	1416.80	27.02	5.93	0.0168
50	–	7.61	–	0.0436
100	695.30	5.67	30.32	0.25
150	580.30	10.9	42.30	0.78
200	778.30	16	70.39	1.61
250	1160.40	–	112.20	–

27.02 Ω to 10.9 Ω, respectively, as the working temperature rises from 20 to 150 °C. Above 150 °C, sensor response gradually increases as the testing temperature increases further. At 20 and 250 °C, the sensor responses peak to its maximum value. Also, the Pt/CNT-COOH based sensor exhibit the highest and the lowest of sensitivity to 20 °C and 150 °C, respectively. The recovery characteristics of these sensors at different temperatures to 1500 ppm H_2S gas have been shown in Table 2. When they are exposed to 20 °C, the recovery times are found 5.93 and 0.0168 Ω/min and they increase as the testing temperature increases further.

4. Conclusions

In this study, the multi-walled CNTs networked films prepared by the CVD process and functionalized with carboxyl and amid groups and decorated with Mo and Pt nanoparticles. The MWCNTs were characterized with SEM/EDX, TEM, XRD, FT-IR and ATR analyses and coated onto low-cost alumina substrates used as gas-sensing nano material for pollutant air monitoring applications, e.g., H_2S gas. MWCNTs and metal functionalizations of the CNTs tangled bundles enhance the gas sensitivity best compared to CNT-COOH and CNT-$CONHC_{18}H_{37}$ based sensors for H_2S gas at room temperature, i.e., Pt/CNT-COOH and Mo/CNT based sensors show a response S of 306.3 Ω and 310.24 Ω to 200 ppm and 539.5 Ω and 805.9 Ω to 1500 ppm H_2S gas, respectively. Low response of CNTs-based sensors to H_2S gas is observed for CNT-COOH based sensor and higher response of CNTs-based sensors to H_2S gas is observed for Mo/CNT and Pt/CNT-COOH based sensors at room temperature. Thus, Interface discrete band-gap states in the p-type semiconducting nanotubes induced by metallic nanoclusters at the surface of the CNTs generate additional charge transfer between nanotubes bundles and gas molecules to enhance the gas sensitivity of the CNTs based sensors. In this work, rapid sensor-regeneration has not been achieved at room temperature for these sensors. However the studies are focusing on rapidly sensor regeneration methodologies, selectivity, optimization of initial resistance and increasing of sensitivity for H_2S gas CNTs-bases sensors at low concentrations.

References

[1] J.W. Gardner, P.N. Bartlett, Sensors & Sensory Systems for an Electronic Nose, Kluwer Academic Publishers, Dordrecht, 1992.
[2] J.R. Li, J.R. Xu, M.Q. Zhang, M.Z. Rong, Carbon black/polystyrene composites as candidates for gas sensing materials, Carbon 41 (2003) 2353–2360.
[3] P. Sharma, P. Ahuja, Recent advances in carbon nanotube-based electronics, Material Research Bulletin 43 (2008) 2517–2526.
[4] A. Liu, Towards development of chemosensors and biosensors with metal-oxide-based nanowires or nanotubes, Biosensors Bioelectronics 24 (2008) 167–177.
[5] J.N. Anker, W.P. Hall, O. Lyandres, N.C. Shah, J.N.C. Zhao, R.P. Van Duyne, Biosensing with plasmonic nanosensors, Nature Material 7 (2008) 442–453.
[6] R.G. Smith, N. D'Souza, S. Nicklin, et al., A review of biosensors and biologically-inspired systems for explosives detection, The Analyst 133 (5) (2008) 571–584.
[7] A. Rudnitskaya, A. Legin, Sensor systems, electronic tongues and electronic noses, for the monitoring of biotechnological processes, Journal of Industrial Microbiology & Biotechnology 35 (5) (2008) 443–451.
[8] I.D. Kim, A. Rothschild, B.G. Lee, D.Y. Kim, S.M. Jo, H.L. Tuller, Ultrasensitive chemiresistors based on electrospun TiO_2 nanofibers, Nano Letters 6 (2006) 2009–2013.
[9] E. Comini, Metal oxide nano-crystals for gas sensing, Analytical Chimica Acta 568 (2006) 28–40.
[10] N. Duc Hoa, N. Van Quy, Y. Cho, D. Kim, Porous single-wall carbon nanotube films formed by in situ arc-discharge deposition for gas sensors application, Sensors and Actuators B 135 (2009) 656–663.
[11] K.J. Donovan, T. Lutz, Macroscopic scale separation of metallic and semiconducting nanotubes by dielectrophoresis, Carbon 43 (2005) 2508–2513.
[12] M. Shiraishi, M. Ata, Work function of carbon nanotubes, Carbon 39 (2001) 1913–1917.
[13] T. Belin, F. Epron, Characterization methods of carbon nanotubes: a review, Materials Science and Engineering B 119 (2005) 105–118.
[14] M. Ouyang, J.L. Huang, C.M. Lieber, Fundamental electronic properties and applications of single-walled carbon nanotubes, Accounts of Chemical Research 35 (2002) 1018–1025.
[15] H. Dai, Carbon nanotubes: synthesis, integration and properties, Accounts of Chemical Research 35 (2002) 1035–1044.
[16] M.S. Dresselhaus, G. Dresselhaus, A. Jorio, A.G. Souza Filho, M.A. Pimenta, R. Saito, Single nanotube Raman spectroscopy, Accounts of Chemical Research 35 (2002) 1070–1078.
[17] Y. Saito, G. Dresselhause, M.S. Dresselhause, Physical Properties of Carbon Nanotubes, Imperial College Press, London, UK, 1998.
[18] J. Kong, N.R. Franklin, C. Zhou, M.G. Chapline, S. Peng, K. Cho, H. Dai, Nanotube molecular wires as chemical sensors, Science 287 (2000) 622–625.
[19] J.P. Novak, E.S. Snow, E.J. Houser, D. Park, J.L. Stepnowski, R.A. McGill, Nerve agent detection using networks of single walled carbon nanotubes, Applied Physics Letters 83 (19) (2003) 4026–4028.
[20] S. Chopra, K. McGuire, N. Gothard, A.M. Rao, A. Pham, Selective gas detection using a carbon nano tube sensor, Applied Physics Letters 83 (2003) 2280–2282.
[21] J. Li, Y. Lu, Q. Ye, M. Cinke, J. Han, M. Meyyappan, Carbon nanotube sensors for gas and organic vapor detection, Nano Letters 3 (7) (2003) 929–933.

[22] L. Valentini, I. Armentano, J.M. Kenny, C. Cantalini, L. Lozzi, S.1. Santucci, Sensors for sub-ppm NO_2 gas detection based on carbon nanotube thin film, Applied Physics Letters 82 (2003) 961–963.
[23] M. Penza, G. Cassano, R. Rossi, A. Rizzo, M.A. Signore, M. Alvisi, N. Lisi, E. Serra, R. Giorgi, Effect of growth catalysts on gas sensitivity in carbon nanotube film based chemiresistive sensors, Applied Physics Letters 90 (2007) 103101.
[24] S. Kim, H.R. Lee, Y.J. Yun, S. Ji, K. Yoo, W.S. Yun, J.Y. Koo, D.H. Ha, Effects of polymer coating on the adsorption of gas molecules on carbon nanotube networks, Applied Physics Letters 91 (2007) 093126.
[25] J.K. Abraham, B. Philip, A. Witchurch, V.K. Varadan, C.C. Reddy, A compact wireless gas sensor using a carbon nanotube/PMMA thin film chemiresistor, Smart Materials & Structures 13 (2004) 1045–1049.
[26] K. Besteman, J. Lee, F. Wiertz, H. Heering, C. Dekker, Enzyme-coated carbon nanotubes as single-molecule biosensor, Nano Letters 3 (6) (2003) 727–730.
[27] M. Penza, R. Rossi, M. Alvisi, G. Cassano, M.A. Signore, E. Serra, R. Giorgi, Pt- and Pd-nanoclusters functionalized carbon nanotubes networked films for sub-ppm gas sensors, Sensors and Actuators B 135 (2008) 289–297.
[28] Y.X. Liang, Y.J. Chen, T.H. Wang, Low-resistance gas sensors fabricated from multiwalled carbon nanotubes coated with a thin tin oxide layer, Applied Physics Letters 85 (2004) 666–668.
[29] P. Qi, O. Vermesh, M. Grecu, A. Javey, Q. Wang, H. Dai, S. Peng, K.J. Cho, Toward large arrays of multiplex functionalized carbon nanotube sensors for highly sensitive and selective molecular detection, Nano Letters 3 (3) (2003) 347–351.
[30] E. Bekyarova, M. Davis, T. Burch, M.E. Itkis, B. Zhao, S. Sunshine, R.C. Haddon, Chemically functionalized single-walled carbon nanotubes as ammonia sensors, Journal of Physical Chemistry B 108 (51) (2004) 19717–19720.
[31] T. Zhang, S. Mubeen, E. Bekyarova, B.Y. Yoo, R.C. Haddon, N.V. Myung, M.A. Deshusses, Poly(m-aminobenzene sulfonic acid) functionalized single-walled carbon nanotubes based gas sensor, Nanotechnology 18 (2007) 165504.
[32] J. Kong, M.G. Chapline, H. Dai, Functionalized carbon nano tubes for molecular hydrogen sensors, Advanced Materials 13 (18) (2001) 1384–1386.
[33] Y.M. Wong, W.P. Kang, J.L. Davidson, A. Wisitsora-at, K.L. Soh, A novel microelectronic gas sensor utilizing carbon nanotubes for hydrogen gas detection, Sensors and Actuators B 93 (2003) 327–332.
[34] M. Penza, G. Cassano, R. Rossi, M. Alvisi, A. Rizzo, M.A. Signore, Th. Dikonimos, E. Serra, R. Giorgi, Enhancement of sensitivity in gas chemiresistors based on carbon nanotube surface functionalized with noble metal (Au, Pt) nanoclusters, Applied Physics Letters 90 (2007) 173123.
[35] A.M. Rashidi, M.M. Akbarnejad, A.A. Khodadadi, Y. Mortazavi, A. Ahmadpour, Single-wall carbon nanotubes synthesized using organic additives to Co–Mo catalysts supported on nanoporous MgO, Nanotechnology 18 (2007) 315605.
[36] S.S. Kish, A. Rashidi, H.R. Aghabozorg, L. Moradi, Increasing the octane number of gasoline using functionalized carbon nanotubes, Applied Surface Science 256 (2010) 3472–3477.
[37] R.-J. Wu, J.-G. Wu, M.-R. Yu, T.-K. Tsai, C.-T. Yeh, Promotive effect of CNT on Co_3O_4–SnO_2 in a semiconductor-type CO sensor working at room temperature, Sensors and Actuators B: Chemical 131 (2008) 306–312.
[38] R.-J. Wu, C.-H. Hu, C.-T. Yeh, P.-G. Su, Nanogold on powdered cobalt oxide for carbon monoxide sensor, Sensors and Actuators B: Chemical 96 (2003) 596–601.
[39] R.-J. Wu, J.-G. Wu, T.-K. Tsai, C.-T. Yeh, Use of cobalt oxide CoOOH in a carbon monoxide sensor operating at low temperatures, Sensors and Actuators B: Chemical 120 (2006) 104–109.
[40] D.W.H. Fam, A.I.Y. Tok, Al. Palaniappan, P. Nopphawan, A. Lohani, S.G. Mhaisalkar, Selective sensing of hydrogen sulphide using silver nanoparticle decorated carbon nanotubes, Sensors and Actuators B: Chemical 138 (2009) 189–192.
[41] S. Peng, K. Cho, P. Qi, H. Dai, A-b initio study of CNT NO_2 gas sensor, Chemical Physics Letters 387 (2004) 271–276.
[42] J. Zhao, A. Buldum, J. Han, J.P. Lu, Gas molecule adsorption in carbon nanotubes and nanotube bundles, Nanotechnology 13 (2002) 195–200.
[43] B.-Y. Wei, M.-C. Hsu, P.-G. Su, H.-M. Lin, R.-J. Wu, H.-J. Lai, A novel SnO_2 gas sensor doped with carbon nanotubes operating at room temperature, Sensors and Actuators B: Chemical 101 (2004) 81–89.

Nosrat Izadi received her B.Sc. in chemical engineering in 2000 from Shiraz University and her M.Sc. in chemical engineering (kinetic and thermodynamic) from Systan & Baloochestan University in 2003. She is a researcher in Research Institute of Petroleum Industry (RIPI), Iran. Her research activity covers aspects of kinetic, synthesis of nanofibers and sensors.

Ali Morad Rashidi received his M.Sc. in chemical engineering in 2000 and his Ph.D. in Chemical Engineering-Nano in 2007 from University of Tehran. He is now head of Nano Technology Center in Research Institute of Petroleum Industry (RIPI), Iran. His research activity covers many aspects of the synthesis, nanomaterials, carbon nanostructures, nanocomposites, nano-catalysts, nanometals and metal oxides, nano-sensors, functionalization of carbon nanostructures, carbon active and carbon molecular sieve, characterization and chemical-physics of carbon nanostructures and nanomaterials with particular emphasis to catalytic, adsorbent, sensing and so on properties.

Samira Golzardi received B.Sc. degree in material engineering from IUST (Iran University of Science and Technology), Department of Metallurgy and Materials Engineering in 2005 and M.Sc. degree in material engineering from IUST (Iran University of Science and Technology), Department of Metallurgy and Materials Engineering, obtained in 2008. She is a researcher in Research Institute of Petroleum Industry (RIPI), Iran. Her current fields of interest are nanomaterials, electro ceramics and glass-ceramics.

Zeinab Talaei received M.Sc. degree in inorganic chemistry from Tarbiat Modares University in 2005. She is now a Ph.D. student at the Department of Chemistry of Tarbiat Modares University under the supervisions of Prof. A.R. Mahjoub and Prof. A.M. Rashidi. Her research project now focuses on ''Pt/CNTs catalyst for catalytic hydrogenation of nitroaromatic compounds''.

Ali Reza Mahjoub received his M.S. in organic chemistry in 1988 and his Ph.D. in inorganic chemistry in 1993 from University of Berlin, Germany. His research activity covers many aspects of the synthesis, characterization and chemical-physics of metal oxides and nano oxides with particular emphasis to catalytic and photo degradation properties.